Bioorganic Chemistry 90 (2019) 103083

Contents lists available at ScienceDirect

Bioorganic Chemistry

journal homepage: www.elsevier.com/locate/bioorg

Discovery of aromatic amides with triazole-core as potent reversal agents against P-glycoprotein-mediated multidrug resistance

Qianqian Qiu[a,1], Jilan Zhu[a,1], Qiutong Chen[a,1], Ziqian Jiang[a], Jiting Xu[a], Xueting Jiang[a], Wenlong Huang[b,c], Zhongquan Liu[a,*], Jing Ye[a,*], Xiaojuan Xu[a,*]

[a] School of Pharmacy, Jiangsu Provincial Key Laboratory of Coastal Wetland Bioresources and Environmental Protection, Yancheng Teachers' University, Yancheng, PR China

[b] Center of Drug Discovery, State Key Laboratory of Natural Medicines, China Pharmaceutical University, Nanjing, PR China

[c] Jiangsu Key Laboratory of Drug Discovery for Metabolic Disease, China Pharmaceutical University, Nanjing, PR China

ARTICLE INFO

Keywords:
P-glycoprotein
Multidrug resistance
Reversal agents
Click chemistry

ABSTRACT

P-glycoprotein (P-gp)-mediated multidrug resistance (MDR) is a major impediment for clinical cancer therapy. 19 novel aromatic amides with triazole-core as MDR reversal agents were designed and synthesized *via* click chemistry to reverse MDR. Among them, compound **42** was identified as the most promising candidate with high potency (EC_{50} = 78.1 ± 5.4 nM), low cytotoxity (SI > 1282) and persistent duration in reversing doxorubicin (DOX) resistance in K562/A02 cells. **42** also enhanced the potency of other P-gp associated cytotoxic agents with different structures. In further study, remarkably increased intracellular accumulation of Rh123 and DOX in K562/A02 cells was achieved by compound **42**, while CYP3A4 activity had no change by compound **42**. These results indicate that compound **42** as a relatively safe modulator of P-gp-mediated MDR has good potential for further development.

1. Introduction

Multidrug resistance (MDR) is a serious obstacle occurred in clinical cancer chemotherapy, leading to more than 90% of chemotherapy failure [1–4]. Several studies have identified that the primary mechanism of MDR is the overexpression of P-glycoprotein (P-gp/ABCB1/MDR1) in the membranes of resistant cells [5]. P-gp was the first member of the ATP binding cassette (ABC) superfamily identified in 1976 by Ling et al. [6] which plays a significant role in drug efflux from cells. It has the ability to mediate ATP-dependent drug translocation across the plasma membrane against considerable concentration gradients, reducing the effective intracellular accumulation of a variety of chemotherapeutic drugs, finally resulting in MDR to cancer cells [7].

Many chemical modulators have been identified that block the action of P-gp [8–10]. Since the first P-gp inhibitor verapamil (VRP) was discovered in 1981, the development of P-gp inhibitors has been over three decades [11]. In particular, the promising third generation P-gp modulators have specific and effective inhibition of P-gp function, for example, Tariquidar(**1**), WK-X-34(**2**) and HM30181(**3**) (Fig. 1) [12–14]. In these excellent inhibitors, 6,7-dimethoxy-2-phenethyl-1,2,3,4-tetrahydro-isoquinoline is the most characteristic moiety, and considered as the foremost active domain with an efficient role in P-gp inhibition [15]. However, most of these modulators suffer from serious deficiency such as unsatisfactory toxicity, low selectivity or pharmacokinetic interaction [16]. Heretofore, no P-gp modulator has been applied to clinic. HM30181 also named Encequidar is still in Phase II clinical trials, which was considered as the most hopeful candidate. Therefore, HM30181 was selected as the leading compound and one positive control. The exploration of potent P-gp inhibitors with high efficiency and low toxicity for cancer therapy remains an urgent need for MDR [17–19].

Extensive efforts have been devoted to develop further bioactive molecules on the basis of 6,7-dimethoxy-2-phenethyl-1,2,3,4-tetrahydro-

Abbreviations: ABC, ATP binding cassette; P-gp, P-glycoprotein; MDR, multidrug resistance; TMD, transmembrane domain; NBD, nucleotide binding domain; TKI, tyrosine kinase inhibitor; SAR, structure-activity relationship; HPLC, high performance liquid chromatography; DOX, doxorubicin; RF, reversal fold; SI, selective index; VRP, verapamil; PTX, paclitaxel; VLB, vinblastine; DNR, daunorubicin; CTX, cyclophosphamide; PBS, phosphate buffered saline; Rh123, rhodamine 123; MFI, mean fluorescence intensity; DMSO, dimethyl sulfoxide; TFA, trifluoroacetic acid; TLC, thin layer chromatography; DCM, dichloromethane; MTT, 3-(4,5-dimethylthiazol-2-yl)-2,5-diphenyltetrazolium bromide; HUVEC, Human Umbilical Vein Endothelial Cells; FBS, fetal bovine serum

* Corresponding authors at: School of Pharmacy, Jiangsu Provincial Key Laboratory of Coastal Wetland Bioresources and Environmental Protection, Yancheng Teachers' University, Yancheng 224007, PR China.

E-mail addresses: zhq6312@aliyun.com (Z. Liu), yej2017@163.com (J. Ye), xuxj@yctu.edu.cn (X. Xu).

[1] Qianqian Qiu, Jilan Zhu and Qiutong Chen contributed equally as first authors.

https://doi.org/10.1016/j.bioorg.2019.103083
Received 24 April 2019; Received in revised form 5 June 2019; Accepted 20 June 2019
Available online 21 June 2019

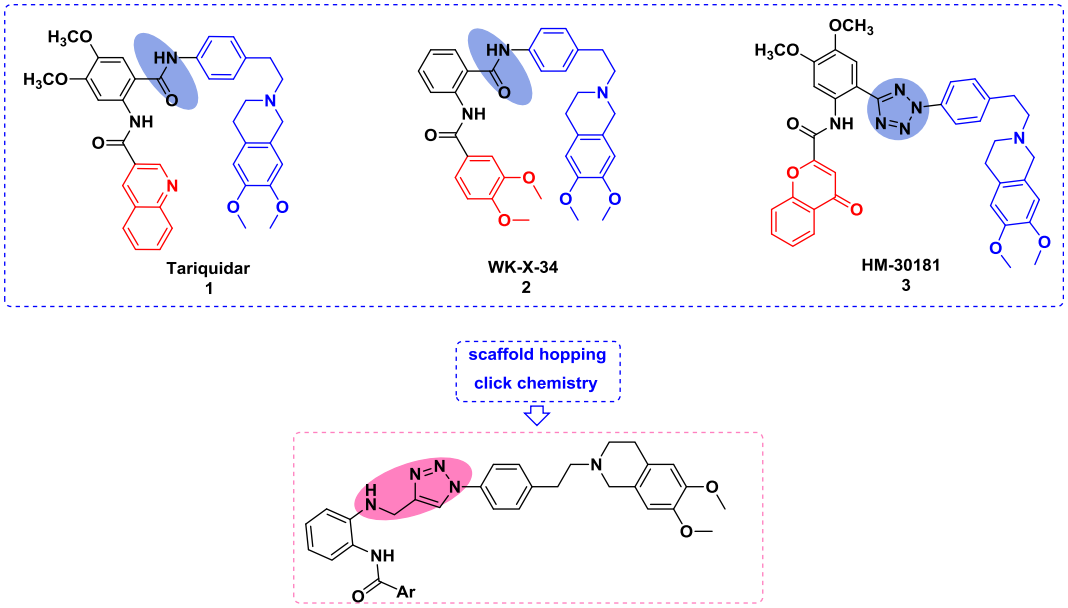

Fig. 1. Structures of the reported potent P-gp inhibitors and design of the target compounds.

isoquinoline [20–22]. Due to the similarity with carboxamide moiety in terms of distance and planarity, 1, 2, 3-triazole ring widely applied in drug discovery is employed as a bioisostere of carboxamide group or tetrazole moiety in the designed compounds by click chemistry, which has better π-π interaction with receptor proteins. It offers high stability even under extreme oxidative and reductive environment and its inclination to form hydrogen bonding elevates its solubility benefiting binding towards biomolecular targets [23–25]. Lipophilicity and presence of aromatic rings are specific physicochemical characteristics in P-gp inhibitors [26]. Hence, substituted benzene rings and heteroaromatic rings were introduced to the hydrophobic domain to develop novel triazole-tetrahydroisoquinoline-core P-gp reversal agents with outstanding affinity to P-gp targets, and high safety profile (Fig. 1) [27].

2. Results and discussion

2.1. Chemistry

As shown in Scheme 1, the series compounds **29–47** with triazol-*N*-phenethyl-tetrahydroisoquinoline were synthesized. Compound **4** was prepared from the starting material 1-fluoro-2-nitrobenzene refluxed in the mixture of DMF with prop-2-yn-1-amine and potassium carbonate for 8 h [28]. Treatment of compound **4** with sodium hyposulfite in 50% ethanol afforded compound **5** which was then reacted with disparate aromatic formic acid in dry dichloromethane with 1-(3-dimethylaminopropyl)-3-ethylcarbodiimide hydrochloride (EDCI), 1-Hydroxybenzotriazole (HOBT) as coupling agents to get the compound **6–24** [29]. Compounds **27** and **28** were synthesized according to literature procedures with minor modification [30,31]. Subsequently, compound **28** and compounds **6–24** were treated with ascorbate sodium and copper sulfate in 75% methanol stirring at room temperature for 48 h to provide compounds **29–47**. Interestingly, some of the target compounds could be precipitated from the reaction solution directly with high purity while the others should be purified by column chromatography. The structures of target compounds obtained were listed in Table 1.

2.2. Biological evaluation

2.2.1. Intrinsic cytotoxicity of target compounds

Since most reported potent P-gp modulators are failed due to toxicity within the therapeutic concentration range, the intrinsic cytotoxicity of target compounds against parental human erythroleukemia sensitive cell line K562 and its DOX-selected derivative P-gp overexpressing K562/A02 cells was evaluated by MTT assay.

As shown in Table 2, the anticarcinogen DOX displayed little inhibitory effect on the survival of K562/A02 cells (IC_{50} of 78.34 ± 3.40 μM) displayed about 113.5-fold greater resistance than K562 cells (IC_{50} = 0.69 ± 0.11 μM). Most of the target compounds had high IC_{50} values with low intrinsic cytotoxicity (IC_{50}s > 100 μM) against both K562 and K562/A02 cells. A few compounds were found to exhibit more toxicity (IC_{50} from 34.48 μM to 68.89 μM) effect on K562/A02 cells than that on sensitive K562 cells, suggesting that these compounds may be more toxic to MDR cells and they were not likely to be substrates of P-gp. The positive control VRP has weak cytotoxic effect toward both two cell lines with IC_{50} values of 32.38 μM and 28.23 μM. On the basis of data points of IC_{50}, the survival rates of 2.0 μM compounds **29–47** were all over 95%, appropriate to determine its reversal effect on MDR cell line. Then the reversal activity of **29–47** in DOX-resistance were evaluated preliminarily in K562/A02 cells at non-toxic concentration of 2.0 μM by MTT.

2.2.2. P-gp modulating activity of the target compounds on reversing DOX resistance in K562/A02 cells and SAR study

Based on the results above, all the target compounds were selected for further reversal study at non-toxic concentration of 2.0 μM. The anticancer drug DOX, the classic P-gp modulator verapamil (VRP) and the lead compound **3** were controls. As the results summarized in Table 3, the anticarcinogen DOX alone displayed little inhibitory effect on the survival of K562/A02 cells (IC_{50} of 78.34 ± 3.40 μM) displayed about 113.5-fold greater resistance than K562 cells (IC_{50} = 0.69 ± 0.11 μM). However, the combination treatment of DOX with most of the target compounds increased the toxic effect. P-gp modulating activity of compounds was evaluated by a parameter known as relative fold (RF). The majority of the target compounds exhibited more active MDR reversal activity than **VRP**, when co-administered with DOX.

According to the data in Table 3, the structure-activity relationship can be summarized as below. Compounds **29–47** with substituent phenyl group all own a comparable reversal activity. Among them, irrespective of electron-withdrawing or -donating groups, the meta-position mono-substituted and unsubstituted compounds exhibited promising reversal potency similar to **3** (compounds **29**, **31**, **35**, **42** and

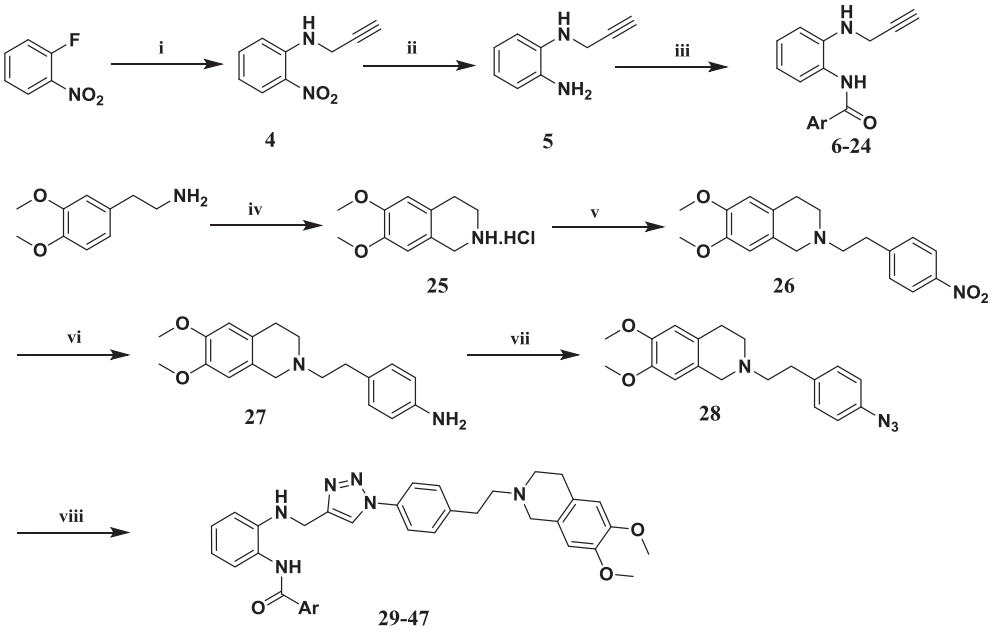

Scheme 1. Synthesis of the target compounds. Reagents and conditions: (i) 2-Propynylamine, K_2CO_3, DMF, 80 °C, 8 h; (ii) $Na_2S_2O_4$, $NaHCO_3$, MeOH: H_2O: THF = 1:1:1, 0 °C ~ r.t., 12 h; (iii) EDCI, HOBT r.t., 24 h; (iv) $(CH_2O)n$, EtOH, r.t., 3 h; con. HCl, reflux, 4 h; (v) 1-(2-bromoethyl)-4-nitrobenzene, K_2CO_3, CH_3CN, reflux, 17 h; (vi) H_2/Pd-C, DCM/EtOH, r.t., 24 h; (vii) $NaNO_2$, 50% AcOH, 0–5 °C, 30 min; NaN_3, 0–5 °C, 50 min; (viii) **6–24**, sodium ascorbate, $CuSO_4$, 75% CH_3OH, 24–48 h.

Table 1
Structures of target compounds.

Compound	Ar	Compound	Ar
29		**39**	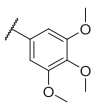
30		**40**	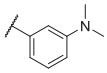
31		**41**	
32		**42**	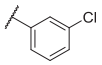
33	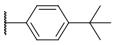	**43**	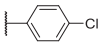
34		**44**	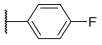
35		**45**	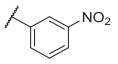
36	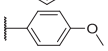	**46**	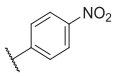
37	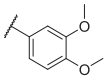	**47**	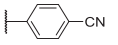
38	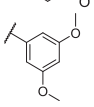		

45), while compound **40** was the exception with low activity caused by the steric hindrance effect of dimethylamino group; the number and the position of methoxyl in the phenyl contributed to the different reversal potency (compounds **34–39**); compared with compounds **37**, the change from benzyl to phenylethyl lead to the lower activity; the ortho- or para-position substituted phenyl compounds with electron-withdrawing or -donating groups (compounds **30**, **32**, **33**, **41**, **43–44** and **46–47**) all displayed minor or no benefit to reversal activity. As a result, compound **42** with a significantly decreased IC_{50} of DOX (1.85 ± 0.10 μM) showed the strongest reversal activity with RF of 42.35, which was superior to **3** and ready for the further studies.

2.2.3. Chemo-sensitizing effect and selective index (SI) of compound 42

Based on the preliminary test, we further investigated the reversal potency of the most potent compound **42** at various concentrations (0.005, 0.01, 0.025, 0.05, 0.075, 0.10, 0.25, 0.50, 1.0 or 2.0 μM) towards K562/A02 cells to get its EC_{50} value. EC_{50} refers to the concentration of inhibitor required to reduce the IC_{50} of DOX by half compared with a control without a modulator [32]. The reversal activity of compound **42** showed apparent dose-dependent manner and still exhibited potent MDR reversal activity (RF = 3.97) when the concentration decreased to 0.1 μM. Additionally, the EC_{50} value of compound **42** was (78.1 ± 5.4) nM (Fig. 2A), which was calculated by GraphPad Prism 6.0 software from the dose response curves. As the most promising compound, the intrinsic cytotoxicity of **42** against normal human gastric epithelial cells (GES-1) was determined to evaluate its safety. The result indicated that **42** showed no cytotoxic effect toward GES-1 cells (IC_{50} > 100 μM) (Fig. 2B). Therefore, the selective index (SI, ratio of IC_{50} toward GES-1 to EC_{50} for reversing DOX resistance) for **42** was very high (SI > 1282), indicating it may be very safe for normal human cells if co-administered with anticancer agents as an MDR modulator.

2.2.4. Effect of 42 on reversing P-gp-mediated resistance to other antineoplastic agents

MDR is accompanied by resistance to other unrelated antineoplastic agents that may own diverse structures and mechanisms of function [33]. Hence, paclitaxel (PTX), vinblastine (VLB), daunorubicin (DNR) and cyclophosphamide (CTX) were chosen to evaluate the capability of **42** on reversing MDR. Fig. 3 reveals clearly that **42** enhanced cytotoxic effects of various agents (PTX, VLB and DNR) related to the P-gp-mediated MDR phenotype in K562/A02 cells but did not affect the potency of non-MDR cytotoxic (as CTX) in the resistant cells. These results suggest that inhibition of P-gp function contributes to the reversal of resistance.

2.2.5. Duration of drug effect

In further evaluation for the duration of action of compound **42**, the experiment was carried out as previously reported [34,35]. The results in Table 4 indicated that the modulating activity was in a wash-time

Table 2
Cytotoxicity of the Target Compounds **29–47** against K562 and K562/A02 Cell Lines.

Compound	IC_{50} (μM)		Compound	IC_{50} (μM)	
	K562	K562/A02		K562	K562/A02
29	> 100	59.15 ± 1.73	**40**	> 100	63.23 ± 2.58
30	> 100	62.19 ± 4.01	**41**	> 100	71.30 ± 2.28
31	> 100	63.06 ± 2.27	**42**	> 100	70.46 ± 2.23
32	> 100	38.71 ± 0.94	**43**	> 100	48.95 ± 3.56
33	72.59 ± 2.82	34.48 ± 2.05	**44**	83.29 ± 5.40	75.34 ± 3.95
34	> 100	89.26 ± 6.03	**45**	> 100	69.35 ± 4.15
35	> 100	> 100	**46**	> 100	> 100
36	> 100	> 100	**47**	73.21 ± 3.74	57.29 ± 3.28
37	> 100	79.64 ± 3.69	VRP	32.38 ± 1.25	28.23 ± 3.17
38	> 100	68.89 ± 3.04	**3**	> 100	> 100
39	> 100	87.56 ± 1.62	DOX	0.69 ± 0.11	78.34 ± 3.40

Table 3
DOX resistance reversal activity of target compounds at 2.0 μM concentration in K562/A02 Cells.

Compound (2.0 μM)	IC_{50}/DOX (μM)	RF	Compound (2.0 μM)	IC_{50}/DOX (μM)	RF
29	3.60 ± 0.17	21.76	**40**	18.61 ± 2.71	4.21
30	15.01 ± 1.23	5.22	**41**	5.82 ± 0.31	13.46
31	3.17 ± 0.17	24.71	**42**	2.19 ± 0.28	35.77
32	4.03 ± 0.58	19.43	**43**	10.66 ± 1.02	8.84
33	12.78 ± 0.75	6.13	**44**	11.30 ± 2.09	6.93
34	8.19 ± 1.01	9.57	**45**	5.12 ± 1.20	15.30
35	3.35 ± 0.26	23.39	**46**	20.30 ± 2.87	3.86
36	9.53 ± 0.93	8.22	**47**	12.24 ± 2.15	6.40
37	5.47 ± 1.09	14.32	VRP (5.0 μM)	15.48 ± 0.50	5.06
38	4.29 ± 0.64	18.26	**3**	2.34 ± 0.21	33.48
39	8.40 ± 1.29	9.33	0.1% DMSO	78.34 ± 3.40	1.00

dependent manner, the longer time, the lower activity. After the removal from the medium, 2.0 μM **3** and **42** persisted significant reversal effect even at 24 h, and **3** exhibited sustaining reversal activity inferior to **42.** However, the action of 5.0 μM VRP continued to exist no more than 6 h. Therefore, it is concluded that the potent reversal effect **42** persisted long time over 24 h after removal from the medium.

2.2.6. *Effect of **42** on accumulation of DOX and Rh123*

Rhodamine-123 (Rh123), a fluorescence specific substrate of P-gp, its fluorescence can be used to monitor the intracellular accumulation level in cells [36,37]. Furthermore, in order to investigate the mechanism of compound **42** in modulating the anticancer drug substrates accumulation level inside K562/A02 cells. The mean fluorescence intensity (MFI) of retained intracellular Rh123 was estimated by BD FACSCalibur flow cytometer through the FL1 tunnel. The classical P-gp inhibitor VRP and **3** were chosen as the positive controls. As the results shown in Fig. 4, K562/A02 cells treated with 2.0 μM **42** and **3**, the MFI of cells increased much more than treated with 5.0 μM VRP. The result indicated that compound **42** was more potent than VRP in Rh123 accumulation in K562/A02 cells, almost had the same efficiency with **3** in enhancing the accumulation of Rh123 in K562/A02 cells.

Furthermore, to validate our assumption that whether the reversal effect of compound **42** is associated with a concomitant increase in DOX accumulation, we utilized fluorescence spectrophotometer to give a further evaluation [38]. When incubated with modulators at various concentrations, the fluorescence intensity of DOX accumulated in K562/A02 cells showed dose-effect dependence. The results demonstrated in Fig. 5 indicated that with the absence of modulators, DOX accumulation in K562 cells was more than 4-fold ($p < 0.01$) than that in K562/A02 cells. In comparison, 0.1 μM compound **42** exhibited similar accumulative activity in K562/A02 compared with 5 μM VRP, and 1.0 μM compound **42** has significantly higher efficiency in enhancing accumulation of DOX than VRP at 5 μM. Meanwhile, 5 μM **3** and **42** showed similar potency in increasing DOX accumulation in K562/A02, almost restored the DOX level to the parental K562′s level. Results indicated that compound **42** was a potent P-gp inhibitor.

2.2.7. *Effect of **42** on cytochrome P3A4 (CYP3A4)*

It is known that P-gp and CYP3A4 have a considerable overlap in the tissue distribution and substrate preference [39]. Several of the second-generation P-gp modulators are substrates for CYP3A4, resulting in unpredictable pharmacokinetic interactions with chemotherapeutic agents. Nevertheless, the new generation P-gp modulators do not affect CYP3A4 at relevant concentrations. In order to further evaluate the safety of **42** as a P-gp modulator, we determined its effect on rat liver CYP3A4 *in vitro*. As shown in Fig. 6, a potent inhibitor of CYP3A4, ketoconazole significantly inhibited the activity of CYP3A4 in a concentration-dependent manner, whereas **42** did not affect the activity of CYP3A4 even at 40 μM, which is much higher than the EC_{50} *in vitro*. The results showed that **42** may be a relatively superior P-gp modulator when coadministered with chemotherapy drugs metabolized by CYP3A4.

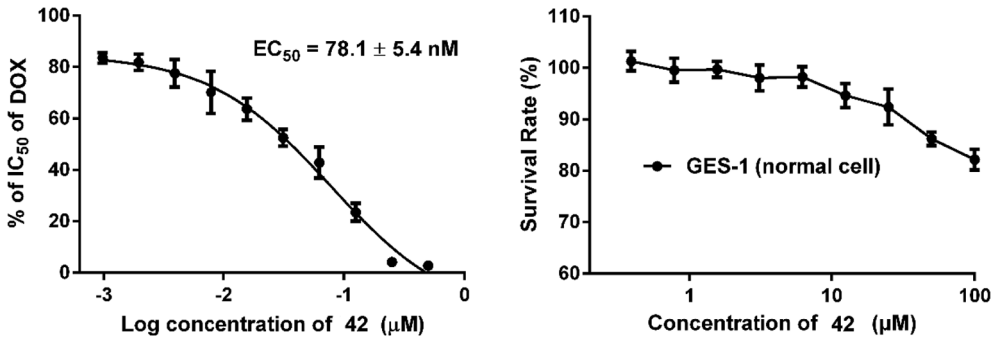

Fig. 2. Impact of **42** on inversing DOX resistance in K562/A02 cells. (A) EC_{50} value for **42** in depressing DOX-resistance of K562/A02 cells. The percentage of DOX IC_{50} was charted with log concentration of **42**, which is equal to (DOX IC_{50} in each modulator concentration/DOX IC_{50} without modulator) × 100%. Thus, EC_{50} can be noted for the modulator concentration, which can diminish the DOX IC_{50} by 50%; (B) Survival rates of **42** at different concentrations were determined in GES-1 cells. Data were analyzed with GraphPad Prism 5.0 software and presented as the mean ± SD of three independent tests.

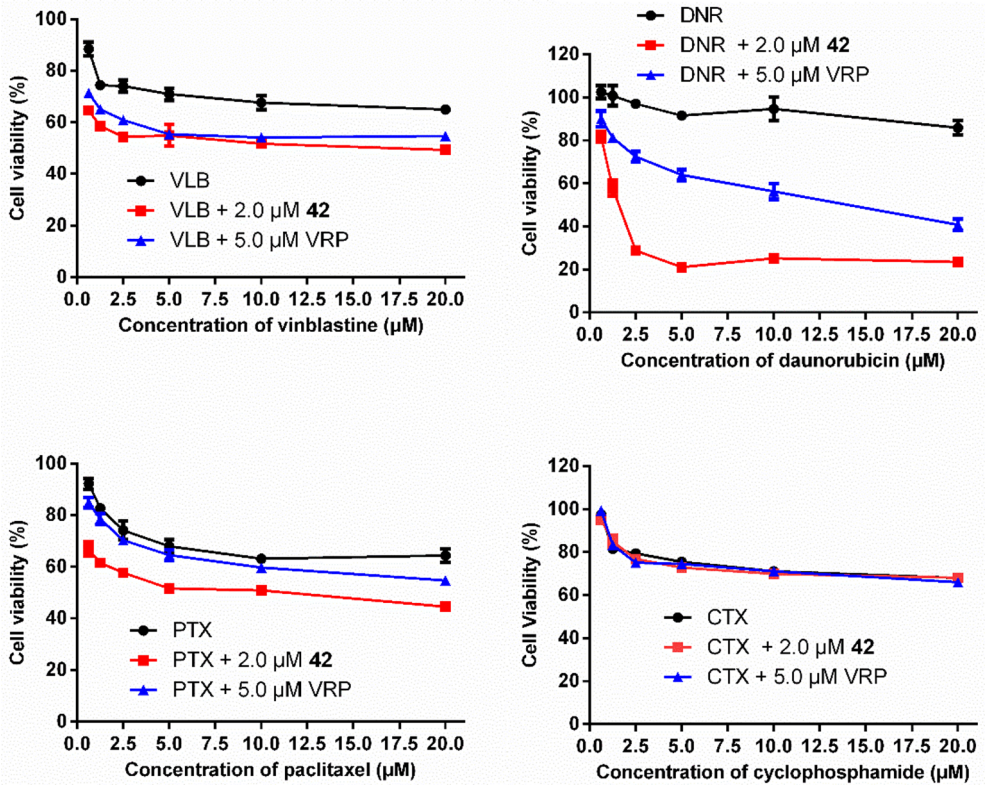

Fig. 3. Reversing potency of **42** on P-gp-mediated resistance to other antineoplastic agents. DNR, PTX, and VLB are P-gp substrates, whereas CTX is not. Each data point is presented as mean ± SD for three independent tests.

3. Conclusion

In the present study, a series of 19 novel aromatic amides with triazole-core as MDR modulators with low cytotoxicity were designed and synthesized based on the click chemistry. All synthesized compounds were evaluated *in vitro* for MDR chemo-sensitizing effects by using the classical P-gp inhibitor VRP as a positive control. Subsequently, the study identified compound **42** was more efficient. Moreover, it did not exhibit toxicity up to 100 μM towards sensitive K562 cells and normal HUVEC cells, which was superior to the lead compound **3**. Additionally, **42** could significantly reverse P-gp-mediated MDR in K562/A02 cells with a dose-dependent manner and possess a considerable potency with EC_{50} = 78.1 ± 5.4 nM. The duration of reversal action of **42** lasted even after 24 h washout.

Moreover, it could remarkably increase the intracellular accumulation of both Rh123 and DOX in K562/A02 cells as well as inhibit their efflux from the cells, which suggested that compound could effectively block the drug efflux function of P-gp. Besides, even at high concentration **42** did not affect the activity of CYP3A4, avoiding the toxicity induced from drug interactions. Therefore, **42** could be served as a promising candidate for the development of P-gp-mediated MDR reversal agents.

4. Experimental section

4.1. General chemistry

All starting materials, reagents and solvents were obtained from commercial sources used without further purification unless otherwise indicated. Column chromatography was carried out on silica gel or alumina (200–300 mesh). Melting points were measured using a RY-1 melting-point apparatus, which was uncorrected. All of the target compounds were analyzed by ^{1}H NMR, ^{13}C NMR (Bruker ACF-300Q, 300 MHz). Chemical shifts are expressed as values (ppm) relative to tetramethylsilane as internal standard and coupling constants (*J* values) were given in hertz (Hz). Abbreviations are used as follows: s = singlet, d = doublet, t = triplet, q = quartet, m = multiplet. LC/MS spectra were recorded on Waters ACQUITY UPLC Systems with Mass (Waters,

Table 4
Duration of MDR reversal in K562/A02 cells after incubation and washout of **VRP**, **3** or **42.**

Treatment schedule	IC_{50}/DOX [μM] (RF)[a]			
	Control	5.0 μM VRP	2.0 μM 3	2.0 μM 42
No wash	82.71 ± 3.94 (1.00)	15.91 ± 2.88 (5.20)	2.64 ± 0.22 (31.33)	2.45 ± 0.32 (33.76)(33.76)
Wash, 0 h	nd[b]	53.02 ± (1.56)	3.67 ± 0.56 (22.54)	4.28 ± 0.29 (19.32)
Wash, 6 h	nd	nd	5.16 ± 0.37 (16.03)	6.39 ± 1.16 (12.94)
Wash, 12 h	nd	nd	7.09 ± 1.04 (11.67)	9.71 ± 1.37 (8.52)
Wash, 24 h	nd	nd	9.85 ± 0.85 (8.40)	15.23 ± 2.34 (5.43)

[a] Numbers in parentheses, Reversal fold (RF), RF = (IC_{50} without modulator)/(IC_{50} with modulator). Each experiment was carried out two to three times, and the values were presented as the mean ± standard error of mean.
[b] nd: not determined.

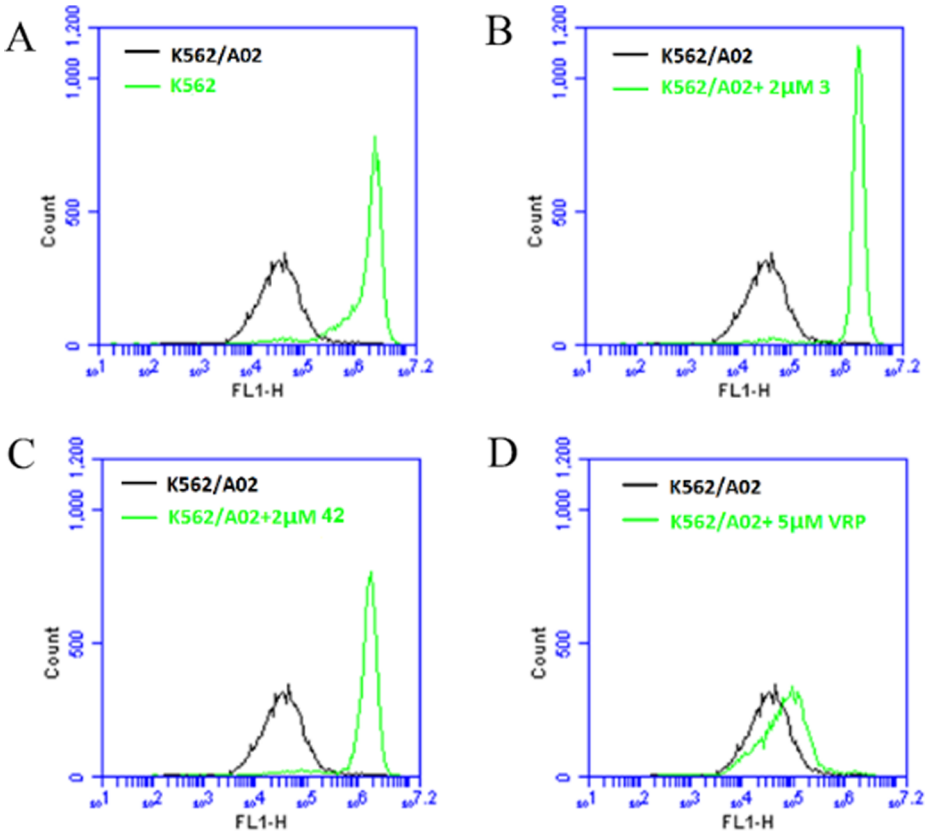

Fig. 4. The effect of target compounds on the Rh123 accumulation in K562 or K562/A02 cells. K562 or K562/A02 Cells were incubated with 5 μM Rh123 without or with 5.0 μM VRP, 2.0 μM **3** or **42** for 150 min at 37 °C before washing with ice PBS for three times. The mean fluorescence intensity (MFI) of retained intracellular Rh123 was measured by BD FACSCalibur flow cytometer through the FL1 tunnel. The shift of the green histogram to the right indicates an increase in intracellular accumulation of Rh123 due to the inhibition of P-gp. (A: K562 and K562/A02 without modulator; B: K562/A02 without modulator or with 2.0 μM **3**; C: K562/A02 without modulator or with 2.0 μM compound **42**; D: K562/A02 without modulator or with 5.0 μM VRP).

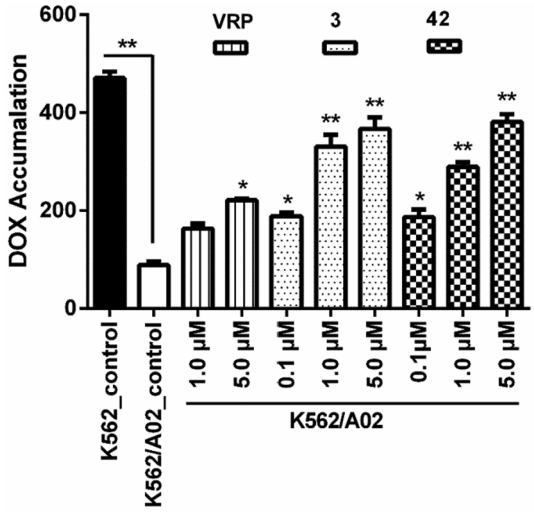

Fig. 5. The effect of target compound on the DOX accumulation in K562 or K562/A02 cells. Cells were incubated with 20 μM DOX with or without various concentrations of **42** or **3** (0.1, 0.5, 2.0 μM) or VRP (0.5, 2.5, 5.0 μM) for 150 min before washing with ice PBS for three times. (A) The cells observed and photographed under a fluorescence microscope. (B) The cells were disintegrated by Triton X100 liquid. The mean fluorescence intensity of retained intracellular DOX was measured by fluorescence spectrophotometer. Data were expressed as means ± SD of three independent experiments. *, $P < 0.05$, **, $P < 0.01$ versus untreated K562/A02 cells. **3** and VRP were used as positive controls while 0.1% DMSO as vehicle control.

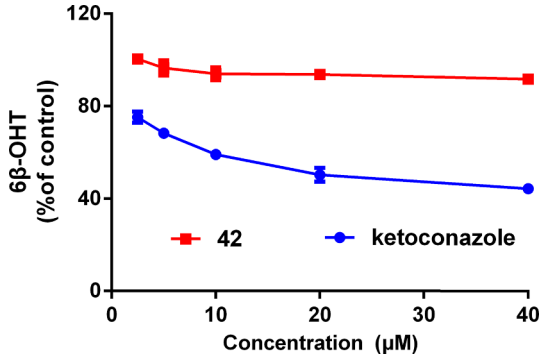

Fig. 6. The effect of **42** and ketoconazole on CYP3A4. Ketoconazole, a specific inhibitor of CYP3A4, was chosen as the positive control. The data represent the mean and SD of three independent experiments.

Milford, MA), ESI-MS were recorded. Thin-layer chromatography (TLC) was performed on GF/UV 254 plates and the chromatograms were visualized under UV light at 254 and 365 nm. Elemental analysis was performed on CHN-O-Rapid instrument and were within 0.4% of the theoretical values unless otherwise noted.

*4.1.1. General procedure for preparation of compounds **29–47***

To the solution of **6–24** (1 mmol) and compound **28** (1 mmol) in 75% methanol (40 mL), ascorbate sodium (30 mg) and $CuSO_4$ (10 mg) were added, respectively to get the target compounds **29–47**.

*4.1.2. N-(2-(((1-(4-(2-(6,7-dimethoxy-3,4-dihydroisoquinolin-2(1H)-yl) ethyl)phenyl)-1H-1,2,3-triazol-4-yl)methyl)amino)phenyl)benzamide(**29**)*

Yield 77.8%; pale yellow solid; m.p.162–164 °C; ESI-MS *m/z*: 589.3 ($[M+H]^+$); ^{1}H NMR (300 MHz, DMSO-d_6) δ ppm: 9.72 (s, 1H), 8.60 (s, 1H), 7.88 (dd, J = 8.5, 7.3 Hz, 5H), 7.61–7.34 (m, 5H), 7.23–7.00 (m, 2H), 6.85 (d, J = 7.9 Hz, 1H), 6.65 (t, J = 8.9 Hz, 3H), 5.71 (s, 1H), 4.46 (s, 2H), 3.69 (s, 6H), 3.54 (s, 2H), 2.88 (s, 2H), 2.69 (s, 6H); ^{13}C NMR (75 MHz, DMSO-d_6) δ ppm: 165.60, 143.16, 141.21, 134.71, 131.39, 130.01, 128.21, 127.81, 127.37, 127.03, 125.83, 120.98, 119.75, 116.21, 111.68, 111.44, 109.87, 55.41, 50.42, 32.25, 28.24; Anal. Calcd for $C_{35}H_{36}N_6O_3$: C, 71.41; H, 6.16; N, 14.28. Found: C,

71.34; H, 6.15; N, 14.25. Purity 97%; t_r 3.80 min; eluent CH_3CN/H_2O 65/35 0.1% FA; fl 1.0 mL/min.

4.1.3. N-(2-(((1-(4-(2-(6,7-dimethoxy-3,4-dihydroisoquinolin-2(1H)-yl) ethyl)phenyl)-1H-1,2,3-triazol-4-yl)methyl)amino)phenyl)-2-methylbenzamide(30)

Yield 79.5%; pale yellow solid; m.p. 133–135 °C; ESI-MS *m/z*: 603.6 ($[M+H]^+$); ^{1}H NMR (300 MHz, DMSO-d_6) δ ppm: 9.61 (s, 1H), 8.64 (s, 1H), 7.73–7.58 (m, 2H), 7.44–7.29 (m, 7H), 7.08 (s, 1H), 6.85–6.63 (m, 4H), 5.56 (s, 1H), 4.45 (s, 2H), 3.69 (s, 8H), 2.87–2.69 (m, 8H), 2.40 (s, 3H); ^{13}C NMR (75 MHz, DMSO-d_6) δ ppm: 168.31, 147.13, 146.88, 146.57, 142.29, 141.25, 135.44, 134.71, 130.45, 130.01, 129.50, 127.42, 126.71, 126.57, 126.35, 125.88, 125.46, 123.88, 121.00, 119.78, 116.43, 111.77, 111.58, 109.96, 59.00, 55.44, 55.03, 50.44, 32.28, 28.25, 19.45; Anal. Calcd for $C_{36}H_{38}N_6O_3$: C, 71.74; H, 6.35; N, 13.94. Found: C, 71.64; H, 6.34; N, 13.91. Purity 97%; t_r 3.93 min; eluent CH_3CN/H_2O 65/35 0.1% FA; fl 1.0 mL/min.

4.1.4. N-(2-(((1-(4-(2-(6,7-dimethoxy-3,4-dihydroisoquinolin-2(1H)-yl) ethyl)phenyl)-1H-1,2,3-triazol-4-yl)methyl)amino)phenyl)-3-methylbenzamide(**31**)

Yield 81.6%; pale yellow solid; m.p. 149–151 °C; ESI-MS *m/z*: 603.4 ($[M+H]^+$); ^{1}H NMR (300 MHz, DMSO-d_6) δ ppm: 9.65 (s, 1H), 8.59 (s, 1H), 7.81–7.72 (m, 4H), 7.46 (d, J = 8.5 Hz, 2H), 7.39 (d, J = 4.5 Hz, 2H), 7.18 (d, J = 7.2 Hz, 1H), 7.09 (t, J = 7.3 Hz, 1H), 6.65 (t, J = 9.0 Hz, 3H), 5.64 (t, J = 5.7 Hz, 1H), 4.45 (d, J = 5.7 Hz, 2H), 3.69 (d, J = 1.6 Hz, 6H), 3.54 (s, 2H), 2.89 (t, J = 7.1 Hz, 2H), 2.70 (s, 6H), 2.38 (s, 3H); ^{13}C NMR (75 MHz, DMSO-d_6) δ ppm: 165.61, 147.12, 146.84, 143.09, 141.23, 137.48, 134.64, 131.94, 130.00, 128.36, 128.11, 127.24, 126.95, 126.57, 125.88, 124.95, 123.92, 120.99, 119.76, 116.29, 111.76, 111.53, 109.95, 59.01, 55.45, 55.03, 50.44, 32.27, 28.26, 20.93; Anal. Calcd for $C_{36}H_{38}N_6O_3$: C, 71.74; H, 6.35; N, 13.94. Found: C, 71.66; H, 6.36; N, 13.95. Purity 97%; t_r 3.95 min; eluent CH_3CN/H_2O 65/35 0.1% FA; fl 1.0 mL/min.

4.1.5. N-(2-(((1-(4-(2-(6,7-dimethoxy-3,4-dihydroisoquinolin-2(1H)-yl) ethyl)phenyl)-1H-1,2,3-triazol-4-yl)methyl)amino)phenyl)-4-methylbenzamide(**32**)

Yield 75.9%; yellow solid; m.p.96–97 °C; ESI-MS *m/z*: 603.1 ($[M+H]^+$); ^{1}H NMR (300 MHz, DMSO-d_6) δ ppm: 9.62 (s, 1H), 8.59 (s, 1H), 7.91 (d, J = 8.0 Hz, 2H), 7.73 (d, J = 8.4 Hz, 2H), 7.46 (d, J = 8.4 Hz, 2H), 7.31 (d, J = 8.0 Hz, 2H), 7.17 (d, J = 7.6 Hz, 1H), 7.08 (t, J = 7.7 Hz, 1H), 6.84 (d, J = 7.7 Hz, 1H), 6.65 (t, J = 8.2 Hz, 3H), 5.64 (t, J = 5.7 Hz, 1H), 4.45 (d, J = 5.7 Hz, 2H), 3.70 (s, 6H), 3.54 (s, 2H), 2.89 (t, J = 7.2 Hz, 2H), 2.71 (s, 6H), 2.38 (s, 3H); ^{13}C NMR (75 MHz, DMSO-d_6) δ ppm: 165.62, 147.12, 146.84, 143.12, 141.27, 134.71, 131.73, 129.99, 128.72, 127.85, 127.30, 126.92, 126.58, 125.88, 123.96, 120.97, 119.75, 116.28, 111.63, 109.95, 59.01, 55.43, 55.04, 50.45, 32.28, 28.25, 20.96; Anal. Calcd for $C_{36}H_{38}N_6O_3$: C, 71.74; H, 6.35; N, 13.94. Found: C, 71.67; H, 6.37; N, 13.92. Purity 96%; t_r 3.97 min; eluent CH_3CN/H_2O 65/35 0.1% FA; fl 1.0 mL/min.

4.1.6. 4-(tert-butyl)-N-(2-(((1-(4-(2-(6,7-dimethoxy-3,4-dihydroisoquinolin-2(1H)-yl)ethyl)phenyl)-1H-1,2,3-triazol-4-yl)methyl) amino)phenyl)benzamide(**33**)

Yield 82.0%; pale grey solid; m.p.150–152 °C; ESI-MS *m/z*: 645.7 ($[M+H]^+$); ^{1}H NMR (300 MHz, DMSO-d_6) δ ppm: 9.63 (s, 1H), 8.60 (s, 1H), 7.95 (d, J = 7.8 Hz, 2H), 7.74 (d, J = 8.0 Hz, 2H), 7.54–7.45 (m, 4H), 7.19 (d, J = 6.7 Hz, 1H), 7.08 (d, J = 7.0 Hz, 1H), 6.85 (d, J = 7.3 Hz, 1H), 6.64 (d, J = 7.6 Hz, 3H), 5.66 (s, 1H), 4.45 (s, 2H), 3.69 (s, 6H), 3.54 (s, 2H), 2.89 (s, 2H), 2.70 (s, 6H), 1.31 (s, 9H); ^{13}C NMR (75 MHz, DMSO-d_6) δ ppm: 165.68, 154.28, 147.01, 143.08, 141.21, 134.72, 131.80, 129.99, 127.71, 127.46, 126.93, 126.58, 125.88, 124.97, 123.96, 120.97, 119.75, 116.29, 111.63, 109.96, 59.02, 55.43, 55.04, 50.45, 34.60, 32.28, 30.90, 28.26; Anal. Calcd for $C_{39}H_{44}N_6O_3$: C, 72.64; H, 6.88; N, 13.03. Found: C, 72.54; H, 6.89; N, 13.01. Purity 99%; t_r 4.03 min; eluent CH_3CN/H_2O 65/35 0.1% FA; fl 1.0 mL/min.

4.1.7. N-(2-(((1-(4-(2-(6,7-dimethoxy-3,4-dihydroisoquinolin-2(1H)-yl) ethyl)phenyl)-1H-1,2,3-triazol-4-yl)methyl)amino)phenyl)-2-methoxybenzamide(**34**)

Yield 78.2%; brown solid; m.p.79–81 °C; ESI-MS *m/z*: 619.6 ($[M+H]^+$); ^{1}H NMR (300 MHz, DMSO-d_6) δ ppm: 9.64 (s, 1H), 8.67 (s, 1H), 8.05–7.82 (m, 3H), 7.64–7.35 (m, 6H), 7.30–6.96 (m, 3H), 6.64 (d, J = 7.3 Hz, 3H), 5.48 (s, 1H), 4.45 (s, 2H), 3.83 (s, 3H), 3.69 (s, 6H), 3.55 (s, 2H), 2.92 (s, 2H), 2.71 (s, 6H); ^{13}C NMR (75 MHz, DMSO-d_6) δ ppm: 164.61, 157.33, 147.97, 147.44, 146.97, 142.84, 141.85, 135.20, 134.47, 132.86, 130.66, 127.00, 126.64, 126.36, 125.68, 125.25, 124.09, 121.68, 121.03, 120.27, 117.45, 112.52, 112.15, 110.34, 59.49, 56.31, 55.88, 55.53, 50.93, 32.75, 28.74; Anal. Calcd for $C_{36}H_{38}N_6O_4$: C, 69.88; H, 6.19; N, 13.58. Found: 69.89; H, 6.18; N, 13.55. Purity 99%; t_r 3.77 min; eluent CH_3CN/H_2O 65/35 0.1% FA; fl 1.0 mL/min.

4.1.8. N-(2-(((1-(4-(2-(6,7-dimethoxy-3,4-dihydroisoquinolin-2(1H)-yl) ethyl)phenyl)-1H-1,2,3-triazol-4-yl)methyl)amino)phenyl)-3-methoxybenzamide(35)

Yield 77.1%; yellow solid; m.p.80–82 °C; ESI-MS *m/z*: 619.6 ($[M+H]^+$); ^{1}H NMR (300 MHz, DMSO-d_6) δ ppm: 9.70 (s, 1H), 8.61 (s, 1H), 8.38 (s, 1H), 7.98 (s, 1H), 7.74 (d, J = 8.0 Hz, 1H), 7.59–7.35 (m, 3H), 7.26–7.04 (m, 3H), 6.85 (d, J = 8.0 Hz, 2H), 6.66 (t, J = 8.9 Hz, 3H), 5.68 (s, 1H), 4.51–4.44 (m, 2H), 3.82 (s, 3H), 3.68 (s, 6H), 3.54 (s, 2H), 2.89 (s, 2H), 2.70 (s, 6H); ^{13}C NMR (75 MHz, DMSO-d_6) δ ppm: 166.03, 154.18, 149.65, 148.86, 147.56, 143.67, 136.45, 135.34, 130.51, 129.85, 127.72, 127.02, 126.32, 124.24, 121.50, 120.58, 120.24, 117.72, 116.82, 113.50, 112.08, 110.35, 59.53, 55.82, 50.94, 43.45, 32.75, 28.75; Anal. Calcd for $C_{36}H_{38}N_6O_4$: C, 69.88; H, 6.19; N, 13.58. Found: 69.78; H, 6.17; N, 13.57. Purity 98%; t_r 3.81 min; eluent CH_3CN/H_2O 65/35 0.1% FA; fl 1.0 mL/min.

4.1.9. N-(2-(((1-(4-(2-(6,7-dimethoxy-3,4-dihydroisoquinolin-2(1H)-yl) ethyl)phenyl)-1H-1,2,3-triazol-4-yl)methyl)amino)phenyl)-4-methoxybenzamide(36)

Yield 72.9%; pale brown solid; m.p.123–125 °C; ESI-MS *m/z*: 619.6 ($[M+H]^+$); ^{1}H NMR (300 MHz, DMSO-d_6) δ ppm: 9.55 (s, 1H), 8.59 (s, 1H), 7.99 (d, J = 8.6 Hz, 2H), 7.74 (d, J = 8.3 Hz, 2H), 7.46 (d, J = 8.2 Hz, 2H), 7.17 (d, J = 7.2 Hz, 1H), 7.10–7.03 (m, 3H), 6.84 (d, J = 8.0 Hz, 1H), 6.65 (t, J = 8.1 Hz, 3H), 5.62 (s, 1H), 4.45 (d, J = 5.4 Hz, 2H), 3.83 (s, 3H), 3.69 (s, 6H), 3.54 (s, 2H), 2.88 (d, J = 6.9 Hz, 2H), 2.70 (s, 6H); ^{13}C NMR (75 MHz, DMSO-d_6) δ ppm: 165.25, 161.78, 147.12, 146.87, 143.17, 141.20, 134.71,129.99, 129.71, 127.34, 126.87, 126.67, 126.58, 125.87, 124.10, 120.98, 119.75, 116.30, 113.43, 111.63, 109.96, 59.00, 55.45, 55.02, 50.44, 32.27, 28.25; Anal. Calcd for $C_{36}H_{38}N_6O_4$: C, 69.88; H, 6.19; N, 13.58. Found: 69.81; H, 6.20; N, 13.59. Purity 97%; t_r 3.83 min; eluent CH_3CN/H_2O 65/35 0.1% FA; fl 1.0 mL/min.

4.1.10. N-(2-(((1-(4-(2-(6,7-dimethoxy-3,4-dihydroisoquinolin-2(1H)-yl)ethyl)phenyl)-1H-1,2,3-triazol-4-yl)methyl)amino)phenyl)-3,4-dimethoxybenzamide(37)

Yield 88.5%; pale yellow solid; m.p.76–77 °C; ESI-MS *m/z*: 649.7 ($[M+H]^+$); ^{1}H NMR (300 MHz, DMSO-d_6) δ ppm: 9.60 (s, 1H), 8.61 (s, 1H), 7.75 (d, J = 8.3 Hz, 2H), 7.70–7.51 (m, 2H), 7.47 (d, J = 8.4 Hz, 2H), 7.26–6.96 (m, 3H), 6.87 (d, J = 7.7 Hz, 1H), 6.66 (t, J = 9.6 Hz, 3H), 5.76 (s, 1H), 4.46 (d, J = 5.2 Hz, 2H), 3.83 (s, 6H), 3.70 (s, 6H), 3.55 (s, 2H), 2.90 (s, 2H), 2.70 (s, 6H); ^{13}C NMR (75 MHz, DMSO-d_6) δ ppm: 165.27, 151.50, 148.19, 147.12, 146.80, 143.24, 141.23, 134.71, 129.99, 127.33, 126.94, 127.33,126.62, 125.87, 124.08, 121.09, 119.77, 116.35, 111.67 (d, J = 14.1 Hz), 111.75, 111.57, 111.04, 109.94, 59.01, 55.62, 55.57, 55.02, 50.44, 32.27, 28.24; Anal. Calcd for $C_{37}H_{40}N_6O_5$: C, 68.50; H, 6.21; N, 12.95. Found: C, 68.45; H, 6.22; N,

12.97. Purity 98%; t_r 3.72 min; eluent CH_3CN/H_2O 65/35 0.1% FA; fl 1.0 mL/min.

4.1.11. N-(2-(((1-(4-(2-(6,7-dimethoxy-3,4-dihydroisoquinolin-2(1H)-yl)ethyl)phenyl)-1H-1,2,3-triazol-4-yl)methyl)amino)phenyl)-3,5-dimethoxybenzamide(38)

Yield 88.5%; pale yellow solid; m.p.89–91 °C; ESI-MS *m/z*: 649.5 ($[M+H]^+$); ^{1}H NMR (300 MHz, DMSO-d_6) δ ppm: 9.66 (s, 1H), 8.59 (s, 1H), 7.73 (d, J = 8.4 Hz, 2H), 7.46 (d, J = 8.5 Hz, 2H), 7.24–6.92 (m, 4H), 6.85 (d, J = 8.0 Hz, 1H), 6.75–6.49 (m, 4H), 5.61 (s, 1H), 4.45 (d, J = 5.5 Hz, 2H), 3.80 (s, 6H), 3.69 (d, J = 1.4 Hz, 6H), 3.54 (s, 2H), 3.00–2.81 (m, 2H), 2.72–2.69 (m, 6H); ^{13}C NMR (75 MHz, DMSO-d_6) δ ppm: 160.27, 146.87, 143.17, 141.24, 136.63, 129.99, 127.33, 126.58, 125.88, 123.75, 120.99, 119.77, 116.30, 111.65, 109.95, 105.78, 103.32, 59.02, 55.43, 55.02, 50.44, 32.27, 28.26; Anal. Calcd for $C_{37}H_{40}N_6O_5$: C, 68.50; H, 6.21; N, 12.95. Found: C, 68.44; H, 6.22; N, 12.94. Purity 99%; t_r 3.75 min; eluent CH_3CN/H_2O 65/35 0.1% FA; fl 1.0 mL/min.

4.1.12. N-(2-(((1-(4-(2-(6,7-dimethoxy-3,4-dihydroisoquinolin-2(1H)-yl)ethyl)phenyl)-1H-1,2,3-triazol-4-yl)methyl)amino)phenyl)-3,4,5-trimethoxybenzamide(39)

Yield 80.7%; yellow solid; m.p.171–173 °C; ESI-MS *m/z*: 679.4 ($[M+H]^+$); ^{1}H NMR (300 MHz, DMSO-d_6) δ ppm: 9.70 (s, 1H), 8.61 (s, 1H), 7.74 (d, J = 6.9 Hz, 2H), 7.47 (d, J = 7.1 Hz, 2H), 7.35 (s, 2H), 7.21–7.06 (m, 2H), 6.88 (d, J = 7.3 Hz, 1H), 6.64 (d, J = 6.8 Hz, 3H), 5.60 (s, 1H), 4.46 (s, 2H), 3.85 (s, 6H), 3.75–3.64 (m, 9H), 3.54 (s, 2H), 2.90 (s, 2H), 2.70 (s, 6H); ^{13}C NMR (75 MHz, DMSO-d_6) δ ppm:165.18, 152.52, 147.12, 146.87, 146.76, 143.29, 141.26, 134.71, 130.00, 129.63, 127.24, 126.58, 125.88, 123.83, 121.00, 119.78, 116.34, 111.76, 111.59, 109.95, 105.47, 60.08, 59.01, 56.02, 55.43, 55.03, 50.45, 32.27, 28.25; Anal. Calcd for $C_{38}H_{42}N_6O_6$: C, 67.24; H, 6.24; N, 12.38. Found: C, 67.21; H, 6.23; N, 12.33. Purity 97%; t_r 3.74 min; eluent CH_3CN/H_2O 65/35 0.1% FA; fl 1.0 mL/min.

4.1.13. N-(2-(((1-(4-(2-(6,7-dimethoxy-3,4-dihydroisoquinolin-2(1H)-yl)ethyl)phenyl)-1H-1,2,3-triazol-4-yl)methyl)amino)phenyl)-3-(dimethylamino)benzamide(40)

Yield 81.4%; yellow solid; m.p.99–101 °C; ESI-MS *m/z*: 632.7 ($[M+H]^+$); ^{1}H NMR (300 MHz, DMSO-d_6) δ ppm: 9.60 (s, 1H), 8.59 (s, 1H), 7.74 (d, J = 8.3 Hz, 2H), 7.46 (d, J = 8.3 Hz, 2H), 7.28–7.10 (m, 5H), 6.92–6.79 (m, 2H), 6.64 (d, J = 7.7 Hz, 3H), 5.56 (s, 1H), 4.45 (d, J = 4.8 Hz, 2H), 3.70 (d, J = 1.3 Hz, 6H), 3.55 (s, 2H), 2.94 (s, 8H), 2.70 (s, 6H); ^{13}C NMR (75 MHz, DMSO-d_6) δ ppm: 166.94, 150.73, 147.57, 147.31, 143.59, 141.71, 135.70, 135.20, 130.50, 129.25, 127.73, 127.41, 127.01, 126.32, 124.58, 121.50, 120.25, 116.85, 115.99, 115.65, 112.07, 110.34, 59.54, 55.90, 55.53, 50.94, 32.76, 28.75; Anal. Calcd for $C_{37}H_{41}N_7O_3$: C, 70.34; H, 6.54; N, 15.52. Found: C, 70.31; H, 6.53; N, 15.54. Purity 96%; t_r 3.83 min; eluent CH_3CN/H_2O 65/35 0.1% FA; fl 1.0 mL/min.

4.1.14. 2-chloro-N-(2-(((1-(4-(2-(6,7-dimethoxy-3,4-dihydroisoquinolin-2(1H)-yl)ethyl)phenyl)-1H-1,2,3-triazol-4-yl)methyl)amino)phenyl)benzamide(41)

Yield 84.8%; yellow solid; m.p.110–112 °C; ESI-MS *m/z*: 623.6 ($[M+H]^+$); ^{1}H NMR (300 MHz, DMSO-d_6) δ ppm: 9.81 (s, 1H), 8.65 (s, 1H), 7.81–7.61 (m, 3H), 7.59–7.40 (m, 5H), 7.34 (d, J = 7.0 Hz, 1H), 7.11 (t, J = 7.3 Hz, 1H), 6.86 (d, J = 8.1 Hz, 1H), 6.71–6.62 (m, 3H), 5.47 (t, J = 5.3 Hz, 1H), 4.46 (d, J = 5.3 Hz, 2H), 3.69 (s, 6H), 3.54 (s, 2H), 2.91–2.87 (m, 2H), 2.69 (s, 6H); ^{13}C NMR (75 MHz, DMSO-d_6) δ ppm: 165.53, 146.39, 142.23, 141.26, 136.86, 134.69, 130.95, 130.03, 129.53, 129.11, 127.10, 126.42, 125.82, 123.09, 121.08, 119.77, 116.35, 111.55, 109.85, 59.03, 55.38, 55.02, 50.43, 32.24, 28.23; Anal. Calcd for $C_{35}H_{35}ClN_6O_3$: C, 67.46; H, 5.66; N, 13.49. Found: C, 67.53; H, 5.64; N, 13.47. Purity 96%; t_r 3.98 min; eluent CH_3CN/H_2O 65/35 0.1% FA; fl 1.0 mL/min.

4.1.15. 3-chloro-N-(2-(((1-(4-(2-(6,7-dimethoxy-3,4-dihydroisoquinolin-2(1H)-yl)ethyl)phenyl)-1H-1,2,3-triazol-4-yl)methyl)amino)phenyl)benzamide(42)

Yield 71.8%; yellow solid; m.p.94–96 °C; ESI-MS *m/z*: 623.4 ($[M+H]^+$); ^{1}H NMR (300 MHz, DMSO-d_6) δ ppm: 9.78 (s, 1H), 8.57 (s, 1H), 8.06 (s, 1H), 7.95 (d, J = 6.7 Hz, 1H), 7.74 (d, J = 7.9 Hz, 2H), 7.63 (d, J = 8.2 Hz, 1H), 7.57–7.32 (m, 3H), 7.19–7.01 (m, 2H), 6.82 (d, J = 7.8 Hz, 1H), 6.65 (d, J = 9.3 Hz, 3H), 5.75 (s, 1H), 4.44 (d, J = 5.4 Hz, 2H), 3.69 (s, 8H), 2.99–2.64 (m, 8H); ^{13}C NMR (75 MHz, DMSO-d_6) δ ppm: 164.23, 146.96, 143.30, 136.63, 134.85, 133.04, 131.16, 130.12, 127.69, 127.54, 127.26, 126.60, 123.31, 121.00, 119.83, 116.09, 111.72, 111.38, 109.89, 55.45, 50.18, 32.24, 28.23; Anal. Calcd for $C_{35}H_{35}ClN_6O_3$: C, 67.46; H, 5.66; N, 13.49. Found: C, 67.38; H, 5.64; N, 13.51. Purity 99%; t_r 3.99 min; eluent CH_3CN/H_2O 65/35 0.1% FA; fl 1.0 mL/min.

4.1.16. 4-chloro-N-(2-(((1-(4-(2-(6,7-dimethoxy-3,4-dihydroisoquinolin-2(1H)-yl)ethyl)phenyl)-1H-1,2,3-triazol-4-yl)methyl)amino)phenyl)benzamide(43)

Yield 83.0%; yellow solid; m.p.164–166 °C; ESI-MS *m/z*: 623.6 ($[M+H]^+$); ^{1}H NMR (300 MHz, DMSO-d_6) δ ppm: 9.76 (s, 1H), 8.59 (s, 1H), 8.03 (d, J = 7.2 Hz, 2H), 7.74 (d, J = 7.4 Hz, 2H), 7.59 (d, J = 7.4 Hz, 2H), 7.46 (d, J = 7.6 Hz, 2H), 7.28–7.00 (m, 2H), 6.84 (d, J = 7.7 Hz, 1H), 6.64 (d, J = 7.5 Hz, 3H), 5.75 (s, 1H), 4.46 (s, 2H), 3.69 (s, 6H), 3.54 (s, 2H), 2.89 (s, 2H), 2.70 (s, 6H); ^{13}C NMR (75 MHz, DMSO-d_6) δ ppm:164.73, 146.86, 143.25, 141.22, 129.90, 128.25, 128.25, 127.47, 127.20, 125.85, 123.46, 120.98, 119.75, 116.15, 111.74, 111.41, 109.92, 59.03, 55.44, 55.03, 50.44, 32.27, 28.26; Anal. Calcd for $C_{35}H_{35}ClN_6O_3$: C, 67.46; H, 5.66; N, 13.49. Found: C, 67.52H, 5.65; N, 13.51. Purity 98%; t_r 4.03 min; eluent CH_3CN/H_2O 65/35 0.1% FA; fl 1.0 mL/min.

4.1.17. N-(2-(((1-(4-(2-(6,7-dimethoxy-3,4-dihydroisoquinolin-2(1H)-yl)ethyl)phenyl)-1H-1,2,3-triazol-4-yl)methyl)amino)phenyl)-4-fluorobenzamide(44)

Yield 80.1%; grey solid; m.p.110–112 °C; ESI-MS *m/z*: 607.6 ($[M+H]^+$); ^{1}H NMR (300 MHz, DMSO-d_6) δ ppm: 9.75 (s, 1H), 8.60 (s, 1H), 8.09 (s, 2H), 7.74 (d, J = 6.6 Hz, 2H), 7.47 (s, 2H), 7.35 (s, 2H), 7.17–7.09 (m, 2H), 6.86 (s, 1H), 6.65 (s, 2H), 5.75 (s, 1H), 4.46 (s, 2H), 3.69 (s, 6H), 3.54 (s, 2H), 2.89 (s, 2H), 2.70 (s, 6H); ^{13}C NMR (75 MHz, DMSO-d_6) δ ppm: 164.72, 147.12, 146.87, 143.25, 141.21, 131.06, 130.52, 130.00, 127.47, 127.12, 126.55, 125.87, 123.62, 120.97, 119.75, 116.17, 115.24, 114.95, 111.76, 111.42, 109.95, 59.00, 55.42, 55.01, 50.42, 32.25, 28.22; Anal. Calcd for $C_{35}H_{35}FN_6O_3$: C, 69.79; H, 5.82; N, 13.85. Found: C, 69.74; H, 5.83; N, 13.83. Purity 98%; t_r 3.91 min; eluent CH_3CN/H_2O 65/35 0.1% FA; fl 1.0 mL/min.

4.1.18. N-(2-(((1-(4-(2-(6,7-dimethoxy-3,4-dihydroisoquinolin-2(1H)-yl)ethyl)phenyl)-1H-1,2,3-triazol-4-yl)methyl)amino)phenyl)-3-nitrobenzamide(45)

Yield 73.7%; yellow solid; m.p.126–128 °C; ESI-MS *m/z*: 634.6 ($[M+H]^+$); ^{1}H NMR (300 MHz, DMSO-d_6) δ ppm: 10.08 (s, 1H), 8.85 (s, 1H), 8.59 (s, 1H), 8.44 (t, J = 6.7 Hz, 2H), 7.82 (t, J = 8.0 Hz, 1H), 7.73 (d, J = 8.4 Hz, 2H), 7.45 (d, J = 8.4 Hz, 2H), 7.20–7.01 (m, 2H), 6.85 (d, J = 8.0 Hz, 1H), 6.67–6.62 (m, 3H), 5.87 (t, J = 5.5 Hz, 1H), 4.46 (d, J = 5.5 Hz, 2H), 3.69 (d, J = 1.4 Hz, 6H), 3.54 (s, 2H), 2.90 (d, J = 6.7 Hz, 2H), 2.69 (s, 6H); ^{13}C NMR (75 MHz, DMSO-d_6) δ ppm: ^{13}C NMR (75 MHz, DMSO) δ 164.22, 155.32, 147.11, 146.85, 143.59, 141.58, 137.92, 134.47, 132.31, 130.02, 128.59, 127.02, 126.54, 125.85, 124.81, 122.52, 121.23, 120.90, 120.01, 113.69, 111.74, 109.92, 62.20, 58.98, 55.42, 55.03, 50.43, 32.28, 28.23; Anal. Calcd for $C_{35}H_{35}N_7O_5$: C, 66.34; H, 5.57; N, 15.47. Found: C, 66.24; H, 5.58; N, 15.44. Purity 99%; t_r 3.71 min; eluent CH_3CN/H_2O 65/35 0.1% FA; fl 1.0 mL/min.

*4.1.19. N-(2-(((1-(4-(2-(6,7-dimethoxy-3,4-dihydroisoquinolin-2(1H)-yl)ethyl)phenyl)-1H-1,2,3-triazol-4-yl)methyl)amino)phenyl)-4-nitrobenzamide(**46**)*

Yield 81.3%; brown solid; m.p.147–149 °C; ESI-MS *m/z*: 634.4 ([M + H]$^+$); ^{1}H NMR (300 MHz, DMSO-d_6) δ ppm: 10.00 (s, 1H), 8.59 (s, 1H), 8.36 (d, J = 7.2 Hz, 2H), 8.26 (s, 2H), 7.75 (s, 2H), 7.47 (s, 2H), 7.28–7.00 (m, 2H), 6.87 (s, 1H), 6.65 (s, 3H), 5.84 (s, 1H), 4.47 (s, 2H), 3.69 (s, 6H), 3.54 (s, 2H), 2.89 (s, 2H), 2.70 (s, 6H); ^{13}C NMR (75 MHz, DMSO-d_6) δ ppm: 164.26, 149.02, 146.93, 141.21, 140.33, 130.02, 129.36, 127.55, 125.79, 123.34, 119.73, 116.07, 111.50, 109.81, 55.38, 54.92, 50.36,32.24, 28.20; Anal. Calcd for $C_{35}H_{35}N_7O_5$: C, 66.34; H, 5.57; N, 15.47. Found: C, 66.36; H, 5.55; N, 15.49. Purity 98%; t_r 3.75 min; eluent CH_3CN/H_2O 65/35 0.1% FA; fl 1.0 mL/min.

*4.1.20. 4-cyano-N-(2-(((1-(4-(2-(6,7-dimethoxy-3,4-dihydroisoquinolin-2(1H)-yl)ethyl)phenyl)-1H-1,2,3-triazol-4-yl)methyl)amino)phenyl) benzamide(**47**)*

Yield 76.8%; pale brown solid; m.p.174–176 °C; ESI-MS *m/z*: 614.7 ([M + H]$^+$); ^{1}H NMR (300 MHz, DMSO-d_6) δ ppm: 9.90 (s, 1H), 8.58 (s, 1H), 8.17 (d, J = 7.5 Hz, 2H), 8.02 (d, J = 7.5 Hz, 2H), 7.74 (d, J = 7.5 Hz, 2H), 7.47 (d, J = 7.5 Hz, 2H), 7.26–7.02 (m, 2H), 6.85 (d, J = 7.1 Hz, 1H), 6.65 (d, J = 7.8 Hz, 3H), 5.80 (s, 1H), 4.46 (s, 2H), 3.69–3.59 (m, 8H), 2.90 (s, 2H), 2.72 (s, 6H); ^{13}C NMR (75 MHz, DMSO-d_6) δ ppm: 164.98, 147.62, 147.35, 143.77, 141.50, 139.12, 135.24, 132.76, 130.53, 129.19, 127.91, 126.18, 123.54, 121.55, 120.25, 118.89, 116.56, 114.15, 112.00, 110.32, 59.22, 55.89, 55.89, 50.82, 32.59, 28.68; Anal. Calcd for $C_{36}H_{35}N_7O_3$: C, 70.45; H, 5.75; N, 15.98. Found: C, 70.39; H, 5.73; N, 15.99. Purity 97%; t_r 3.82 min; eluent CH_3CN/H_2O 65/35 0.1% FA; fl 1.0 mL/min.

4.2. Cytotoxicity and MDR reversal assay

The cell viability was tested by MTT assay with a minor modification [40–42]. K562, K562/A02 and GES-1 cells were harvested during logarithmic growth phase, and were seeded in 96-well micro-titer plates at 1 × 10^4 cells per well. In the MTT assay for anticancer MDR reversal experiments, cells were exposed to the presence of anticancer agents (DOX, DNR, VLB, PTX or CTX) with or without P-gp inhibitors for 48 h [30]. MTT dye (10 μl of 2.5 mg/ml in PBS) was added to each well 4 h priors to experiment termination in a 37 °C incubator containing 5% CO_2, the absorbance at 490 nm was read on a microplate reader (Thermo, USA). The IC_{50} values of the compounds for cytotoxicity were calculated by GraphPad Prism 6.0 software (GraphPad software, San Diego, CA, USA) from the dose–response curves.

4.3. Duration of the MDR reversal

The experiment was carried out as the reported procedures with minor modification [30]. In brief, K562/A02 cells were seeded in 96-well micro-titer plates at 1 × 10^4 per well during logarithmic growth phase, cells were incubated for 24 h with or without 2.0 μM of **2**, **3**, **42** or PBS before being washed 0 or 3 times with culture medium. Then, the cells were incubated for 0, 6, 12, or 24 h before the addition of varying concentrations of DOX or vehicle. The incubation was continued for 48 h prior to the MTT assay.

4.4. DOX and Rh123 intracellular accumulation

The reported procedures with minor modification was employed for the detection of accumulation of DOX and Rh123 [43,44]. K562 and K562/A02 cells were seeded into 24-well plates 1.5 × 10^4 per well. Different concentrations of compound **42** and **3** were pre-incubated with cells for 60 min. Then 20 μM DOX (or 5 μM Rh123) was added into each well and incubated for 90 min, washed with ice-cold PBS for three times at 4 °C. The fluorescence intensity of cells can be observed through fluorescence microscope. Afterwards the cells were disintegrated by Triton × 100 liquid. The mean fluorescence intensity (MFI) of accumulation intracellular DOX was measured by fluorescence spectrophotometer. Data were expressed as means ± SD of three independent experiments. The MFI of retained intracellular Rh123 was estimated by BD FACSCalibur flow cytometer through the FL1 tunnel.

4.5. Rh123 efflux assay

K562 and K562/A02 cells were seeded into 24-well plates 1.5 × 10^4 per well and incubated with 5 μM Rh123 for 60 min before washing with ice-cold PBS for three times. Then the cells were incubated with or without various concentrations of compound **42** or **3** (2.0 μM) for another 90 min. Afterwards the cells were washed thrice in ice-cold PBS. Afterwards the cells were disintegrated by Triton × 100 liquid.[44] The MFI of retained intracellular Rh123 was measured by fluorescence spectrophotometer. Data were expressed as means ± SD of three independent experiments.

4.6. Western blotting

After 48 h incubation with VRP (5.0 μM), **3** (2.0 μM), **42** (0.1 μM, 2.0 μM), K562/A02 cells were harvested and washed trice with ice-cold PBS and lysed with RIPA lysis buffer containing 10% PMSF. Total protein was extracted by centrifuging at 12,000r for 15 min at 4 °C. Total protein content was determined by BCA Protein Assay kit. The Protein samples were separated by 8% SDS-PAGE gel electrophoresis and the proteins were transferred to PVDF membranes. Then the membranes were blocked with TBST (10 mM Tris-HCl, pH 7.5, 150 mM NaCl and 0.1% Tween 20) containing 5% nonfat dried milk for 1 h and probed with the specific P-gp antibody, β-tublin antibody overnight at 4 °C. After being washed with TBST 3 times, the membranes were incubated with the secondary antibodies for 2 h at room temperature. After washing for another three times, proteins were visualized using the enhanced chemiluminescence detection system and Quantity One software were used to analyses the protein's band intensity [9,45].

4.7. CYP3A4 assay

Differential centrifugation separated Rat liver microsomes and the protein concentration was determined by the Bradford method [46]. The activity of CYP3A4 was measured with testosterone (substrate of CYP3A4) and HPLC analysis as modified previous description [47,48]. Based on the content of 6β-OH testosterone (6β-OHT), the specific product of testosterone metabolized by CYP3A4, the effect of the target compound on CYP3A4 could be determined [49]. The column used was an octyldecylsilyl (C18) reverse-phase HPLC column (5 mm, 150 mm, 4.6 mm). Column temperature was set to 35 °C. The flow rate was 1.0 mL/min. Mobile phase A consisted of water. Mobile phase B consisted of acetonitrile. From 0 to 7.5 min, the percentage of mobile phase B was 35%, at which time the percentage of mobile phase B was immediately increased to 48%, where it remained until 14 min. At 14 min, the percentage of mobile phase B was returned to 35%, where it remained until the end of the run at 19 min. Detection was by UV absorbance at 245 nm. The liver microsomes were incubated with testosterone (50 mM) in the presence or absence of **42** and ketoconazole, an inhibitor of CYP3A4, as the positive control.

Declaration of Competing Interest

The authors declare no competing financial interest.

Acknowledgements

This study was supported by National Natural Science Foundation of China (No. 81872733, 81872734 and 81803353), Jiangsu Qing Lan Project, and the Foundation of Jiangsu Provincial Key Laboratory of

Coastal Wetland Bioresources and Environmental Protection (No. JKLBS2017011).

Appendix A. Supplementary material

Supplementary data to this article can be found online at https://doi.org/10.1016/j.bioorg.2019.103083.

References

[1] R. Krishna, L.D. Mayer, Multidrug resistance (MDR) in cancer, Eur. J. Pharm. Sci. 11 (4) (2000) 265–283.
[2] X.Q. Li, L. Wang, Y. Lei, T. Hu, F.L. Zhang, C.H. Cho, K.K. To, Reversal of P-gp and BCRP-mediated MDR by tariquidar derivatives, Eur. J. Med. Chem. 101 (2015) 560–572.
[3] L. Quintieri, M. Fantin, C. Vizier, Identification of Molecular Determinants of Tumor Sensitivity and Resistance to Anticancer Drugs, Springer, New York, 2007.
[4] N. Kerru, P. Singh, N. Koorbanally, R. Raj, V. Kumar, Recent advances (2015–2016) in anticancer hybrids, Eur. J. Med. Chem. 142 (2017) 179–212.
[5] Z. Chen, T. Shi, L. Zhang, P. Zhu, M. Deng, C. Huang, T. Hu, L. Jiang, J. Li, Mammalian drug efflux transporters of the ATP binding cassette (ABC) family in multidrug resistance: a review of the past decade, Cancer Lett. 370 (1) (2016) 153–164.
[6] R.L. Juliano, V. Ling, A surface glycoprotein modulating drug permeability in Chinese hamster ovary cell mutants, Biochim. Biophys. Acta 455 (1) (1976) 152–162.
[7] R. Callaghan, F. Luk, M. Bebawy, Inhibition of the multidrug resistance P-glycoprotein: time for a change of strategy? Drug. Metab. Dispos. 42 (4) (2014) 623–631.
[8] A. Palmeira, E. Sousa, M.H. Vasconcelos, M.M. Pinto, Three decades of P-gp inhibitors: skimming through several generations and scaffolds, Curr. Med. Chem. 19 (13) (2012) 1946–2025.
[9] R. Mudududdla, S.K. Guru, A. Wani, S. Sharma, P. Joshi, R.A. Vishwakarma, A. Kumar, S. Bhushan, S.B. Bharate, 3-(Benzo[d][1,3]dioxol-5-ylamino)-N-(4-fluorophenyl)thiophene-2-carboxamide overcomes cancer chemoresistance via inhibition of angiogenesis and P-glycoprotein efflux pump activity, Org. Biomol. Chem. 13 (14) (2015) 4296–4309.
[10] J.B. Bharate, Y.S. Batarseh, A. Wani, S. Sharma, R.A. Vishwakarma, A. Kaddoumi, A. Kumar, S.B. Bharate, Synthesis and P-glycoprotein induction activity of colupulone analogs, Org. Biomol. Chem. 13 (19) (2015) 5488–5496.
[11] T. Tsuruo, H. Iida, S. Tsukagoshi, Y. Sakurai, Overcoming of vincristine resistance in P388 leukemia in vivo and in vitro through enhanced cytotoxicity of vincristine and vinblastine by verapamil, Cancer Res. 41 (5) (1981) 1967–1972.
[12] W. Li, H. Zhang, Y.G. Assaraf, K. Zhao, X.J. Xue, J.B. Xie, D.H. Yang, Z.S. Chen, Overcoming ABC transporter-mediated multidrug resistance: molecular mechanisms and novel therapeutic drug strategies, Drug Resist. Update 27 (2016) 14–29.
[13] V. Jekerle, W. Klinkhammer, D.A. Scollard, K. Breitbach, R.M. Reilly, M. Piquette-Miller, M. Wiese, In vitro and in vivo evaluation of WK-X-34, a novel inhibitor of P-glycoprotein and BCRP, using radio imaging techniques, Int. J. Cancer 119 (2) (2010) 414–422.
[14] T.E. Kim, N. Gu, S.H. Yoon, J.Y. Cho, K.M. Park, S.G. Shin, I.J. Jang, K.S. Yu, Tolerability and pharmacokinetics of a new P-glycoprotein inhibitor, HM30181, in healthy Korean male volunteers: single- and multiple-dose randomized, placebo-controlled studies, Clin. Ther. 34 (2) (2012) 482–494.
[15] M.L. Pati, C. Abate, M. Contino, S. Ferorelli, R. Luisi, L. Carroccia, M. Niso, F. Berardi, Deconstruction of 6,7-dimethoxy-1,2,3,4-tetrahydroisoquinoline moiety to separate P-glycoprotein (P-gp) activity from σ 2 receptor affinity in mixed P-gp/σ 2 receptor agents, Eur. J. Med. Chem. 89 (4) (2015) 691–700.
[16] Z. Binkhathlan, A. Lavasanifar, P-glycoprotein inhibition as a therapeutic approach for overcoming multidrug resistance in cancer: current status and future perspectives, Curr. Cancer Drug Targets 13 (3) (2013) 326–346.
[17] F.J. Sharom, Complex interplay between the P-glycoprotein multidrug efflux pump and the membrane: its role in modulating protein function, Front. Oncol. 4 (2014) 41.
[18] C. Yang, I.L. Wong, K. Peng, Z. Liu, P. Wang, T. Jiang, T. Jiang, L.M. Chow, S.B. Wan, Extending the structure-activity relationship study of marine natural ningalin B analogues as P-glycoprotein inhibitors, Eur. J. Med. Chem. 125 (2017) 795–806.
[19] C.Y. Chen, C.M. Lin, H.C. Lin, C.F. Huang, C.Y. Lee, T.C.S. Tou, C.C. Hung, C.S. Chang, Structure − activity relationship study of novel 2-Aminobenzofuran derivatives as P-glycoprotein inhibitors, Eur. J. Med. Chem. 125 (2016) 1023–1035.
[20] H. Müller, I.K. Pajeva, C. Globisch, M. Wiese, Functional assay and structure-activity relationships of new third-generation P-glycoprotein inhibitors, Bioorg. Med. Chem. 16 (5) (2008) 2448–2462.
[21] G. Nesi, N.A. Colabufo, M. Contino, M.G. Perrone, M. Digiacomo, R. Perrone, A. Lapucci, M. Macchia, S. Rapposelli, SAR study on arylmethyloxyphenyl scaffold: looking for a P-gp nanomolar affinity, Eur. J. Med. Chem. 76 (7) (2014) 558–566.
[22] Q. Qiu, B. Liu, J. Cui, Z. Li, X. Deng, H. Qiang, J. Li, C. Liao, B. Zhang, W. Shi, Design, synthesis, and pharmacological characterization of N-(4-(2 (6, 7-dimethoxy-3, 4-dihydroisoquinolin-2 (1 h) yl) ethyl) phenyl) quinazolin-4-amine derivatives: novel inhibitors reversing P-glycoprotein-mediated multidrug resistance, J. Med. Chem. 60 (8) (2017) 3289–3302.
[23] D. Dheer, V. Singh, R. Shankar, Medicinal attributes of 1,2,3-triazoles: current developments, Bioorg. Chem. 71 (2017) 30–54.
[24] T. Muller, S. Brase, Click chemistry finds its way into covalent porous organic materials, Angew. Chem. Int. Edit. 50 (50) (2011) 11844–11845.
[25] D. Astruc, L.Y. Liang, A. Rapakousiou, J. Ruiz, Click dendrimers and triazole-related aspects: catalysts, mechanism, synthesis, and functions. A bridge between dendritic architectures and nanomaterials, Acc. Chem. Res. 45 (4) (2012) 630–640.
[26] F.J. Sharom, The P-glycoprotein multidrug transporter, Essays Biochem. 50 (1) (2011) 161–178.
[27] L. Zhang, Z. Zhang, F. Chen, Y. Chen, Y. Lin, J. Wang, Aromatic heterocyclic esters of podophyllotoxin exert anti-MDR activity in human leukemia K562/ADR cells via ROS/MAPK signaling pathways, Eur. J. Med. Chem. 123 (2016) 226–235.
[28] D.N. Kommi, P.S. Jadhavar, D. Kumar, A.K. Chakraborti, "All-water" one-pot diverse synthesis of 1, 2-disubstituted benzimidazoles: hydrogen bond driven 'synergistic electrophile–nucleophile dual activation'by water, Green Chem. 15 (3) (2013) 798–810.
[29] S. Aichhorn, M. Himmelsbach, W. Schöfberger, Synthesis of quinoxalines or quinolin-8-amines from N-propargyl aniline derivatives employing tin and indium chlorides, Org. Biomol. Chem. 13 (36) (2015) 9373–9380.
[30] B. Liu, Q. Qiu, T. Zhao, L. Jiao, J. Hou, Y. Li, H. Qian, W. Huang, Discovery of novel P-glycoprotein-mediated multidrug resistance inhibitors bearing triazole core via click chemistry, Chem. Biol. Drug. Des. 84 (2) (2014) 182–191.
[31] L. Jiao, Q. Qiu, B. Liu, T. Zhao, W. Huang, H. Qian, Design, synthesis and evaluation of novel triazole core based P-glycoprotein-mediated multidrug resistance reversal agents, Bioorg. Med. Chem. 22 (24) (2014) 6857–6866.
[32] K.F. Chan, I.L. Wong, J.W. Kan, C.S. Yan, L.M. Chow, T.H. Chan, Amine linked flavonoid dimers as modulators for P-glycoprotein-based multidrug resistance: structure-activity relationship and mechanism of modulation, J. Med. Chem. 55 (5) (2012) 1999–2014.
[33] R. Dastvan, S. Mishra, Y.B. Peskova, R.K. Nakamoto, RK2, H.S. Mchaourab, Mechanism of allosteric modulation of P-glycoprotein by transport substrates and inhibitors, Science 364 (6441) (2019) 689–692.
[34] P. Mistry, A.J. Stewart, W. Dangerfield, S. Okiji, C. Liddle, D. Bootle, J.A. Plumb, D. Templeton, P. Charlton, In vitro and in vivo reversal of P-glycoprotein-mediated multidrug resistance by a novel potent modulator, XR9576, Cancer Res. 61 (2) (2001) 749–758.
[35] B. Liu, Q. Qiu, T. Zhao, L. Jiao, Y. Li, W. Huang, H. Qian, 6,7 Dimethoxy 2 2 [4 (1H 1,2,3 triazol 1 yl)phenyl]ethyl 1,2,3,4 tetrahydroisoquinolines as superior reversal agents for P glycoprotein mediated multidrug resistance, Chemmedchem 10 (2) (2015) 336–344.
[36] V. Munic, Z.L. Kelneric, H.V. Erakovic, Differences in assessment of macrolide interaction with human MDR1 (ABCB1, P-gp) using rhodamine-123 efflux, ATPase activity and cellular accumulation assays, Eur. J. Pharm. Sci. 41 (1) (2010) 86–95.
[37] M.D. Perloff, E. Störmer, L.L. von Moltke, D.J. Greenblatt, Rapid assessment of P-glycoprotein inhibition and induction in vitro, Pharm. Res. 20 (8) (2003) 1177–1183.
[38] Y. Kang, R.R. Perry, Effect of alpha-interferon on P-glycoprotein expression and function and on verapamil modulation of doxorubicin resistance, Cancer Res. 54 (11) (1994) 2952–2958.
[39] T. Tachibana, M. Kato, J. Takano, Y. Sugiyama, Predicting drug-drug interactions involving the inhibition of intestinal CYP3A4 and P-glycoprotein, Curr. Drug Metab. 11 (9) (2010) 762–777.
[40] S. Jabbar, P.R. Twentyman, J.V. Watson, The MTT assay underestimates the growth inhibitory effects of interferons, Br. J. Cancer 60 (4) (1989) 523–528.
[41] L.W. Fu, Y.M. Zhang, Y.J. Liang, X.P. Yang, Q.C. Pan, The multidrug resistance of tumour cells was reversed by tetrandrine in vitro and in xenografts derived from human breast adenocarcinoma MCF-7/adr cells, Eur. J. Cancer 38 (3) (2002) 418–426.
[42] W. Ning-Ning, Z. Li-Jun, W. Li-Nan, H. Ming-Feng, Q. Jun-Wei, Z. Yi-Bing, Z. Wan-Zhou, L. Jie-Shou, W. Jin-Hua, Mechanistic analysis of taxol-induced multidrug resistance in an ovarian cancer cell Line, Asian Pac. J. Cancer Prev. 14 (9) (2013) 4983–4988.
[43] I.L. Wong, K.F. Chan, K.H. Tsang, C.Y. Lam, Y. Zhao, T.H. Chan, L.M. Chow, Modulation of multidrug resistance protein 1 (MRP1/ABCC1)-mediated multidrug resistance by bivalent apigenin homodimers and their derivatives, J. Med. Chem. 52 (17) (2009) 5311–5322.
[44] P.R. Twentyman, T. Rhodes, S. Rayner, A comparison of rhodamine 123 accumulation and efflux in cells with P-glycoprotein-mediated and MRP-associated multidrug resistance phenotypes, Eur. J. Cancer 30A (9) (1994) 1360–1369.
[45] Y.J. Wang, R.J. Kathawala, Y.K. Zhang, A. Patel, P. Kumar, S. Shukla, K.L. Fung, S.V. Ambudkar, T.T. Talele, Z.S. Chen, Motesanib (AMG706), a potent multikinase inhibitor, antagonizes multidrug resistance by inhibiting the efflux activity of the ABCB1, Biochem. Pharmacol. 90 (4) (2014) 367–378.
[46] M. Bradford, A rapid and sensitive method for the quantization of microgram quantities of protein utilizing the principle of protein dye binding, Anal. Biochem. 72 (s 1–2) (1976) 248–254.
[47] B.H. Hellum, O.G. Nilsen, In vitro inhibition of CYP3A4 metabolism and P-glycoprotein-mediated transport by trade herbal products, Basic Clin. Pharmacol. Toxicol. 102 (5) (2010) 466–475.
[48] C.L. Dai, H.Y. Xiong, L.F. Tang, X. Zhang, Y.J. Liang, M.S. Zeng, L.M. Chen, X.H. Wang, L.W. Fu, Tetrandrine achieved plasma concentrations capable of reversing MDR in vitro and had no apparent effect on doxorubicin pharmacokinetics in mice, Cancer Chemother. Pharmacol. 60 (5) (2007) 741–750.
[49] D. Dai, J. Tang, R. Rose, E. Hodgson, R.J. Bienstock, H.W. Mohrenweiser, J.A. Goldstein, Identification of variants of CYP3A4 and characterization of their abilities to metabolize testosterone and chlorpyrifos, J. Pharmacol. Exp. Ther. 299 (3) (2001) 825–831.